Atmos. Chem. Phys., 18, 7527–7537, 2018
https://doi.org/10.5194/acp-18-7527-2018

Atmospheric Chemistry and Physics Open Access EGU

Gas chromatography using ice-coated fused silica columns: study of adsorption of sulfur dioxide on water ice

Stefan Langenberg[1,a] **and Ulrich Schurath**[2]

[1]Institut für Physikalische und Theoretische Chemie, University of Bonn, Bonn, Germany
[2]Institut für Umweltphysik, University of Heidelberg, Heidelberg, Germany
[a]now at: Klinik und Poliklinik für Hals-Nasen-Ohrenheilkunde/Chirurgie, University of Bonn, Bonn, Germany

Correspondence: Stefan Langenberg (langenberg@uni-bonn.de)

Received: 27 August 2017 – Discussion started: 1 December 2017
Revised: 23 April 2018 – Accepted: 26 April 2018 – Published: 30 May 2018

Abstract. The well established technique of gas chromatography is used to investigate interactions of sulfur dioxide with a crystalline ice film in a fused silica wide bore column. Peak shape analysis of SO_2 chromatograms measured in the temperature range 205–265 K is applied to extract parameters describing a combination of three processes: (i) physisorption of SO_2 at the surface, (ii) dissociative reaction with water and (iii) slow uptake into bulk ice. Process (ii) is described by a dissociative Langmuir isotherm. The pertinent monolayer saturation capacity is found to increase with temperature. The impact of process (iii) on SO_2 peak retention time is found to be negligible under our experimental conditions.

By analyzing binary chromatograms of hydrophobic *n*-hexane and hydrophilic acetone, the premelt surface layer is investigated in the temperature range 221–263 K, possibly giving rise to irregular adsorption. Both temperature dependencies fit simple van't Hoff equations as expected for process (i), implying that irregular adsorption of acetone is negligible in the investigated temperature range. Adsorption enthalpies of -45 ± 5 and -23 ± 2 kJ mol^{-1} are obtained for acetone and *n*-hexane.

The motivation of our study was to assess the vertical displacement of SO_2 and acetone in the wake of aircraft by adsorption on ice particles and their subsequent sedimentation. Our results suggest that this transport mechanism is negligible.

1 Introduction

Adsorption of SO_2 on ice surfaces is of interest in the chemistry and physics of the troposphere and stratosphere. In particular, large ice particles in contrails have been shown by lidar soundings to settle fairly rapidly (Schumann, 1994). This gave rise to speculations that sedimentation of ice particles provides a significant mechanism for the vertical displacement of SO_2 and possibly other adsorbing trace gases, particularly in the upper troposphere. An analogous mechanism has been addressed for the absorption and desorption of SO_2 in raindrops falling through the plume of a power station (Walcek and Pruppacher, 1983). Therefore, Langenberg (1997) investigated the adsorption of the water-soluble aircraft exhaust ingredients SO_2 and acetone on ice over a wide temperature range. The data were interpreted in terms of a simple Langmuir model: SO_2 is weakly adsorbed at the normal ice surface and much more strongly adsorbed at active surface sites. Huthwelker et al. (2006) and Crowley et al. (2010) found that the results of Langenberg were in disagreement with the work of Clegg and Abbatt (2001) and other investigators: in contrast to these studies, Langenberg's analysis implied a classical temperature dependence, i.e., more SO_2 being adsorbed at lower temperatures. In addition, the surface coverage derived from the data of Langenberg (1997) is about an order of magnitude lower than implied by the data of Clegg and Abbatt (2001). Therefore, we have reanalyzed the experiments of Langenberg (1997) using more sophisticated linear and nonlinear regression techniques using R (R Core Team, 2016). The experimental results and their reanalysis are published in the peer-reviewed literature for the first time.

The interaction of SO_2 with ice can be separated into fast and much slower components, as summarized by Huthwelker et al. (2006), Abbatt (2003) and Crowley et al. (2010). In the works of Chu et al. (2000) and Clegg and Abbatt (2001) the fast interaction was investigated. Both used low pressure flow tubes interfaced with a mass spectrometer to measure SO_2. The former studied vapor-deposited ice coatings, while the latter used ice that was prepared by freezing a liquid water film. The experiments of Chu et al. (2000) were performed under non-equilibrium conditions on a timescale < 10 ms, revealing an initial uptake coefficient of $\gamma = 10^{-5}$ for SO_2 at 191 K.

Clegg and Abbatt (2001) measured adsorption/desorption bursts of SO_2 on ice in the range 213–238 K using SO_2 partial pressures between 10^{-5} and 10^{-3} Pa in helium. They could show that the equilibrium amount of SO_2 adsorbed on ice was scaled with the square root of its partial pressure above the surface. They concluded that the square root dependence results from fast dissociative adsorption of SO_2 at the ice surface:

$$SO_2 + 2H_2O \rightleftharpoons H_3O^+ + HSO_3^-. \quad \text{(R1)}$$

Experiments on timescales that are orders of magnitude longer, utilizing packed ice columns in the temperature range 213–270 K (Clapsaddle and Lamb, 1989; Sommerfeld and Lamb, 1986; Conklin et al., 1993; Conklin and Bales, 1993), have revealed that SO_2 is eventually incorporated in ice and partially oxidized to H_2SO_4. The uptake rate increases with temperature and with a dependence that is less than linear on the SO_2 partial pressure. The experimental data were reanalyzed and interpreted by Huthwelker et al. (2001) in terms of SO_2 diffusing into an internal reservoir. For various reasons the packed column experiments were not suitable to study fast reversible adsorption on ice.

A long-standing issue in studies of gas–ice surface interactions is the possible involvement of a premelt layer (Bartels-Rausch et al., 2014). It is now well established that an extended quasi-liquid layer exists at the surface of pure water ice at temperatures of a few kelvins below the melting point (Dash et al., 2006).

We employed a chromatographic technique to study adsorption of SO_2: ice was deposited as the stationary phase as a thin film of 2–8 µm thickness in a fused silica wide bore column (diameter $2r = 530\,\mu\text{m} \pm 10\,\%$, length 10 m). Adsorption on the ice surface was studied by injecting small amounts of the trace gas under study spiked with a non-adsorbing tracer into the column. Due to adsorption, the trace gas was retained for the adjusted retention time t_n relative to the non-adsorbing tracer. Therefore, the inert tracer and the trace gas under study were separated and two peaks appear at the column outlet, where they were detected by a suitable detector. The t_n value was obtained from the peak maxima.

The slope of the adsorption isotherm was determined by the peak maxima method of gas chromatography (Huber and Gerritse, 1971): from t_n and the column void time t_0, the capacity ratio k' was measured as a function of partial pressure p of the trace gas under investigation. When using a capillary column with cylindrical geometry, k' is related to the slope of the isotherm by

$$k' = \frac{t_n}{t_0} = \left(\frac{\partial n_{ad}}{\partial n_g}\right) = \frac{2\,RT}{r}\left(\frac{\partial q}{\partial p}\right), \quad (1)$$

where t_0 is calculated from the column dimensions, the carrier gas mass flow rate and the column head pressure; see e.g., Langenberg et al. (1998) and Giddings (1991). It follows from Eq. (1) that if the isotherm is convex (like the Langmuir adsorption isotherm), the slope of which continuously decreases with increasing concentration, segments of the peak with high concentrations move faster through the column than at low concentrations. Therefore, the resulting chromatographic peak exhibits tailing.

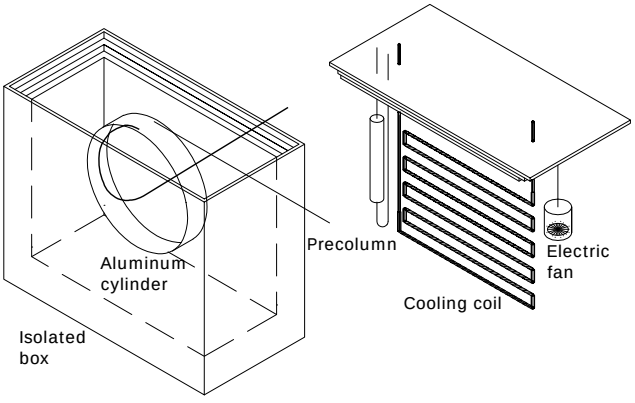

Figure 1. Expanded view of the box used for the coating procedure. Inside the box the air is recirculated by a fan (Micronel) to avoid temperature gradients. The temperature is monitored with two Pt100 sensors mounted at the top and bottom of the box.

2 Experimental

Langenberg and Schurath (1999) already described the coating procedure in detail: a constant volume flow of air ($p = 1$–2 bar) was bubbled through a water reservoir at room temperature and admitted into the column maintained at 205–220 K. At the same time the column was slowly drawn through a pinhole into a cold box by a rotating aluminum drum inside the box which was driven by a stepping motor; see Fig. 1. The box was cooled by a recirculating thermostat (Lauda RLS 6) with a useful temperature range $T \geq 205$ K regulated to ± 1 K. The end of the fused silica column which was fixed to the aluminum drum was connected to a Teflon tube which was led out of the box through the axis of the aluminum cylinder. By slowly drawing the column into the cold box, the water vapor condensed and froze. If the winding speed v and the water vapor mass flow $\dot{m}(H_2O)$ into the column are

held constant, the theoretical film thickness h of a compact ice layer is given by

$$h = \frac{\dot{m}(H_2O)}{2\pi r v \rho(H_2O)}, \quad (2)$$

where $\rho(H_2O)$ is the ice density. In this way ice films of 2–8 µm thickness and ca. 8 m length could be prepared.

After finishing the coating procedure, the ice-coated column was operated like an ordinary gas chromatography column, with synthetic air as the carrier gas. The flow rate was varied by means of a flow controller (ASM 10–100 sccm), while the column head pressure was monitored with a pressure transducer. The carrier gas from the flow controller was humidified using a precolumn filled with water saturated silica gel that was mounted inside the same cold box.

Although the carrier gas was humidified to match the vapor pressure over ice inside the cold box, the ice film slowly but unavoidably is degraded by sublimation due to carrier gas decompression along the length of the column. Since the carrier gas was pre-humidified to 100 % relative humidity with respect to ice at each experimental temperature, the net evaporation rate from the ice surface is zero at the column head, but increases along the column. The rate of ice film thickness degradation $\dot{h}$ is given by

$$\dot{h} = \frac{V_m \dot{n} p(H_2O)}{2\pi r l}\left(\frac{1}{p_o} - \frac{1}{p_i}\right), \quad (3)$$

where p_i is the column head pressure, p_o the pressure at the column exit, l the length of the coated part of the column, $\dot{n}$ the carrier gas mass flow and $V_m = 2 \times 10^{-5}\,m^3\,mol^{-1}$ the molar volume of water ice. At 265 K, $p_i = 2$ bar, $p_o = 1$ bar, $\dot{n} = 7.85 \times 10^{-5}\,mol\,s^{-1}$ (≈ 100 sccm) yields $\dot{h} = 0.7\,\mu m\,h^{-1}$. Vapor pressure $p(H_2O)$ over ice is taken from Wexler (1977).

Some experiments were carried out using aged ice films: after column preparation, the carrier gas was interrupted and the column was kept at 265 K overnight.

Void fused silica columns (SGE) are commercially available either with a pristine silica surface or with a methylsilyl-deactivated surface. Pristine silica surfaces are less hydrophobic than methylsilyl-deactivated silica surfaces. Wetting of the two column types was investigated by contact angle measurements using the capillary rise method (Bartle et al., 1981; Ogden and McNair, 1986). For non-wettable surfaces, the contact angle is $\vartheta > 90°$ and for wettable surfaces it is $\vartheta < 90°$. For the untreated column $\vartheta = 63 \pm 1°$ and for the methylsilyl-deactivated column $\vartheta = 111 \pm 1°$ was found. To remove ionic impurities, the columns were rinsed with Milli-Q water prior to each coating procedure. The experiments were performed, using methylsilyl-deactivated columns unless otherwise indicated. We expected that using the methylsilyl-deactivated columns, interactions of the trace gas with the uncoated part of the column could be minimized. After each coating procedure, series of concentration-dependent chromatograms at two or three constant temperatures were recorded. The temperature was increased in steps of about 15 K, keeping the column for 1 h at each new temperature to achieve thermal equilibrium. In our studies of SO_2 adsorption the peak partial pressure was in the range $p = 0.001$–1 Pa at the column exit.

10–500 µl dilute mixtures of the compound under study and an appropriate inert tracer were injected with a gastight syringe. Mixtures of SO_2 (≈ 220 ppmv) and SF_6 (≈ 50 ppmv) as a tracer in air were used. A modified Bendix flame photometric sulfur monitor (Farwell and Barinaga, 1986) was utilized. For the hydrocarbon experiments, a mixture of acetone (180 ppmv) and methane (55 ppmv) or *n*-hexane (120 ppmv) and methane (55 ppmv) in air was injected in the column. They were monitored using a Carlo Erba flame ionization detector (FID), whereby methane was used as a non-adsorbable tracer. The detector signal was amplified by a Keithley microvoltmeter and recorded by a computer.

Due to experimental constraints, about 1 m of the column inside the box remained uncoated. In order to exclude artifacts from this ice-free section, the adsorption of SO_2 in a totally ice-free column was also investigated. The obtained k' values ranged from 0.35 to 0.45 at 219 K and from 0.15 to 0.25 at 234 K. At $T > 248$ K SO_2 and SF_6 could no longer be separated. Thus, interference by the 1 m ice-free column may be neglected for the lower concentration range of the isotherm.

3 Results

3.1 Adsorption of SO_2

For low concentrations the retention times of SO_2 are strongly dependent on the amount of SO_2 injected. The peaks exhibit strong tailing, even at low $p(SO_2)$; see Fig. 2a.

For further analysis, the peak maximum method (Huber and Gerritse, 1971) is applied to determine $(\partial q/\partial p)$ as a function of p: it is assumed that Eq. (1) applies to the peak maximum, an assumption which is verified afterwards by the peak shape calculation; see discussion.

The most simplistic model for adsorption is Henry's adsorption isotherm: the surface concentration q as a function of the gas partial pressure p is given by

$$q = K_H p \quad (4)$$

($[K_H] = mol\,m^{-2}\,Pa^{-1}$). After applying Eq. (1), we arrive at

$$k' = \frac{2\,RT}{r} K_H. \quad (5)$$

If adsorption of a compound is properly described by Henry's adsorption isotherm, the adjusted retention times should be independent of $p(SO_2)$ and thus of the amount of adsorbing gas injected in our experiments. This is obviously

Table 1. Nonlinear fit of the experimental data with the humidified carrier gas and $h > 4\,\mu m$ to different models. The binary variable ν denotes if the column was aged ($\nu = 1$) or not ($\nu = 0$).

Model	Model parameters	P	Residual standard error
Temkin + Henry	$\zeta = (a_1 + a_2 T)(1 + a_3 \nu)$		0.1977
Eq. (8)	$a_1 = -(9 \pm 1) \times 10^{-9}\,\mathrm{mol\,m^{-2}}$	< 0.01	
	$a_2 = (4.8 \pm 0.5) \times 10^{-11}\,\mathrm{mol\,m^{-2}K^{-1}}$	< 0.01	
	$a_3 = 0.6 \pm 0.2$	< 0.01	
	$K_H = (1.11 \pm 0.08) \times 10^{-8}\,\mathrm{mol\,m^{-2}\,Pa^{-1}}$	< 0.01	
Langmuir + Henry	$K_L = a_1 \exp(a_2/T)$		0.2066
Eq. (11)	$q_S = a_3(1 + a_4 \nu)$		
	$a_1 = (9 \pm 13) \times 10^{-16}\,\mathrm{mol\,m^{-2}\,Pa^{-1}}$	0.49	
	$a_2 = (5 \pm 0.4) \times 10^{3}\,\mathrm{K}$	< 0.01	
	$a_3 = (1.10 \pm 0.08) \times 10^{-8}\,\mathrm{mol\,m^{-2}}$	< 0.01	
	$a_4 = 0.9 \pm 0.2$	< 0.01	
	$K_H = (1.60 \pm 0.08) \times 10^{-8}\,\mathrm{mol\,m^{-2}\,Pa^{-1}}$	< 0.01	
Langmuir (dissociation) + Henry	$q_S = a_1 \exp(a_2/T)(1 + a_3 \nu)$		0.1938
Eq. (17)	$a_1 = (5 \pm 3) \times 10^{-6}\,\mathrm{mol\,m^{-2}}$	0.02	
	$a_2 = -(1.3 \pm 0.1) \times 10^{3}\,\mathrm{K}$	< 0.01	
	$a_3 = 0.6 \pm 0.2$	< 0.01	
	$K_{I1} K_H = (7 \pm 5) \times 10^{-14}\,\mathrm{mol^2\,m^{-4}\,Pa^{-1}}$	0.1	
	$K_H = (1.35 \pm 0.01) \times 10^{-8}\,\mathrm{mol\,m^{-2}\,Pa^{-1}}$	< 0.01	

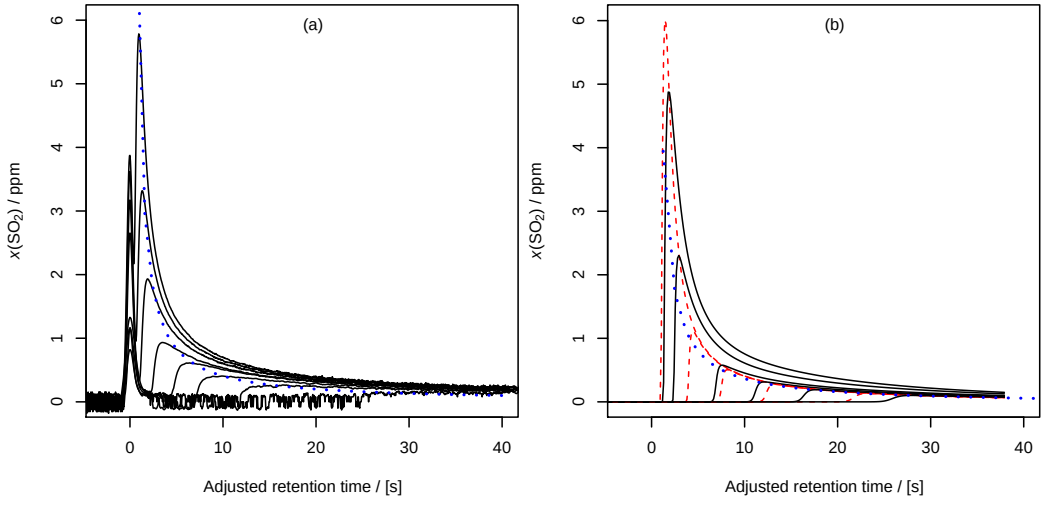

Figure 2. (a) Chromatograms from injection of various amounts of a SF_6 / SO_2 mixture at 247 K and 2 µm ice film thickness. **(b)** Simulated SO_2 chromatograms using the Temkin isotherm with $\zeta = 4.3 \times 10^{-9}\,\mathrm{mol\,m^{-2}}$, $K_T = 10^{-6}\,\mathrm{mol\,m^{-2}\,Pa^{-1}}$ and $K_H = 2.8 \times 10^{-9}\,\mathrm{mol\,m^{-2}\,Pa^{-1}}$ using 100 cells in an axial direction. Dashed lines: simulation without absorption/diffusion into the solid phase. Solid lines: simulation including diffusion into the solid phase with $H = 50$ and $D_s = 2 \times 10^{-13}\,\mathrm{m^2\,s^{-1}}$ using 30 cells in a radial direction. The dotted lines are calculated with Eq. (1). They represent the locations of the experimental peak maxima.

only the case for high $p(SO_2)$. However, strong peak tailing is observed, indicating a saturation effect. Using the observed $k' \approx 0.2$, Eq. (5) is used to calculate a tentative $K_H = 1.5 \times 10^{-8}\,\mathrm{mol\,m^{-2}\,Pa^{-1}}$. At $p(SO_2) = 1\,\mathrm{Pa}$ at peak maximum, a surface concentration of $q(SO_2) = 1.5 \times 10^{-8}\,\mathrm{mol\,m^{-2}}$ is obtained using Eq. (4). Clegg and Abbatt (2001) estimated that about $5 \times 10^{14}\,\mathrm{cm^{-2}} = 8.3 \times 10^{-6}\,\mathrm{mol\,m^{-2}}$ molecules of the size of SO_2 can be packed on the surface next to each other. Therefore, surface coverage of the normal ice surface is only $\theta = 0.2\,\%$. Thus, it can be excluded that the normal ice surface is saturated with SO_2 and that SO_2–SO_2 interactions

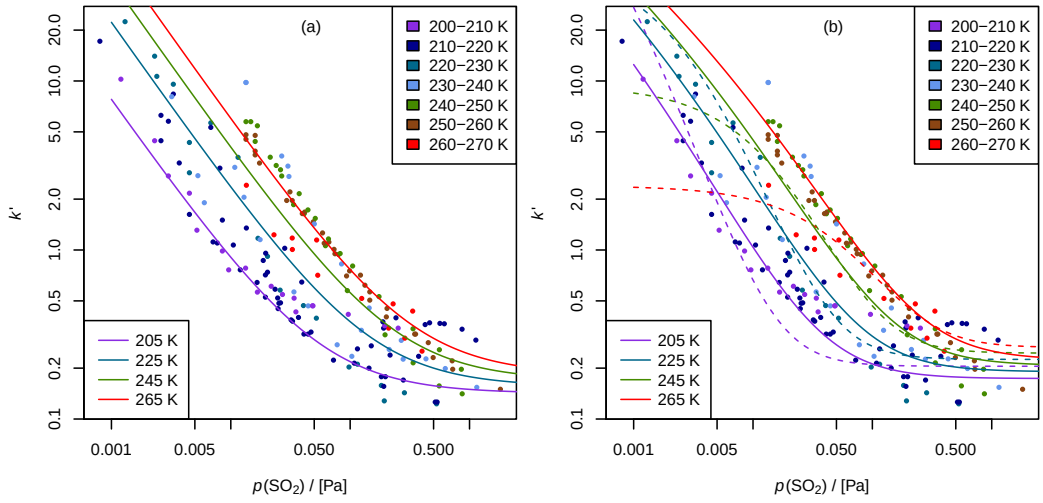

Figure 3. Double logarithmic plot of k' vs. $p(SO_2)$ at peak maximum for experiments with ice film thickness $h > 4\,\mu m$ and without ice aging. **(a)** Fit with Temkin adsorption isotherm according to Eq. (8). **(b)** Fit with simple Langmuir model (dashed lines) according to Eq. (11) and with the dissociative Langmuir model (solid curves) according to Eq. (17).

come into effect. The observed peak tailing must have another cause like adsorption at active sites.

For lower $p(SO_2)$ an additional stronger adsorption mechanism comes into play which yields a $k' \propto p^{-1}$ dependency in the limit $p(SO_2) \to 0$; see Fig. 3. In the low partial pressure range, it is found that k' increases with increasing temperature. An isotherm explaining the $k' \propto p^{-1}$ dependence is the Temkin isotherm

$$q = \zeta \ln\left(\frac{K_T p}{\zeta}\right), \tag{6}$$

($[K_T] = \mathrm{mol\,m^{-2}\,Pa^{-1}}$); see Sect. S1 in the Supplement. The Temkin isotherm assumes that the Gibbs free enthalpy of adsorption decreases linearly with increasing coverage. Inserting the derivative of Eq. (6) in Eq. (1) yields the prevailing pressure dependence in the limit $p \to 0$:

$$k' = \frac{2\,RT}{r}\frac{\zeta}{p}. \tag{7}$$

Together with the weaker physisorption described by Henry's adsorption isotherm of Eq. (5), it follows that

$$k' = \frac{2\,RT}{r}\left(\frac{\zeta}{p} + K_H\right). \tag{8}$$

Note that only the model parameter ζ of the Temkin isotherm can be determined from concentration-dependent k' measurements. This is because the second model parameter K_T is arbitrarily removed by differentiation of Eq. (6). The linear relationship of k' vs. $1/p$ is used to study the relationship between film thickness, temperature, pre-humidification and column aging, which are treated as independent variables by multiple linear regression using data from 336 chromatograms. Since the retention times at lower concentrations are difficult to obtain due to considerable peak broadening, the obtained k' values are weighted with $1/k'$ in the linear regression.

The results indicate that k' significantly increases with increasing temperature ($P < 0.01$), column aging ($P < 0.01$) and ice film thickness ($P = 0.03$). Therefore, further analysis is confined to a subset of 249 experiments with ice film thickness $h > 4\,\mu m$. All these experiments were performed using a pre-humidified carrier gas.

In this subset, k' significantly increases with temperature ($P < 0.01$) and column aging ($P < 0.01$) but not with ice film thickness ($P = 0.81$). A linear dependency on ζ from T and column aging is formulated; see Table 1. Next, the fit parameters are determined by nonlinear regression of the log-scaled data; see Fig. 3a. The residuals of the fit are normally distributed (Shapiro–Wilk normality test; $P = 0.19$).

Langenberg (1997) applied a Langmuir adsorption model for the chemisorption in addition to a Henry's adsorption isotherm for weak physisorption: the ice surface is assumed to be a solid surface composed of series of active sites capable of binding SO_2. The Langmuir isotherm is defined by the expression

$$\theta = \frac{q}{q_S} = \frac{(K_L/q_S)p}{1 + (K_L/q_S)p} \tag{9}$$

($[K_L] = \mathrm{mol\,m^{-2}\,Pa^{-1}}$), where q_S is the monolayer saturation capacity. For K_L, a van't Hoff-like temperature dependency was assumed. For low p where $(K_L/q_S)p \ll 1$ the Langmuir model simplifies to the Henry's adsorption isotherm $q \approx K_L p$. By applying Eq. (1) to the Langmuir model of Eq. (9), we form

$$k' = \frac{2\,RT}{r}\frac{K_L q_S^2}{(K_L p + q_S)^2} \tag{10}$$

and by adding Henry's law adsorption isotherm arithmetic expression for independent weak physisorption one obtains

$$k' = \frac{2\,RT}{r}\left(\frac{K_{\mathrm{L}} q_{\mathrm{S}}^2}{(K_{\mathrm{L}} p + q_{\mathrm{S}})^2} + K_{\mathrm{H}}\right). \quad (11)$$

When fitting this model to the log-scaled data, the dashed lines in Fig. 3b are obtained with the model parameters listed in Table 1. From these model parameters, an apparent adsorption enthalpy of $\Delta H_{\mathrm{a}} = -(41 \pm 3)\,\mathrm{kJ\,mol^{-1}}$ is estimated. As can be seen in Fig. 3b, the fit is quite good at lower temperatures but fails at higher temperatures. When comparing the fit to those of the Temkin model, it is obvious that the Langmuir model is not appropriate.

Clegg and Abbatt (2001) proposed a model for the adsorption of SO_2 where SO_2 interacts with the ice surface by hydrolyzing, as it does when being dissolved in liquid water. The equilibrium of the first dissociation step of SO_2 in water (see Reaction R1) is described by

$$K_{I1} = \frac{q(\mathrm{H_3O^+})\,q(\mathrm{HSO_3^-})}{q(\mathrm{SO_2})}. \quad (12)$$

On neutral ice, where $q(\mathrm{HSO_3^-}) = q(\mathrm{H_3O^+})$, the surface concentration of S_{IV} is given by

$$q(\mathrm{S_{IV}}) = q(\mathrm{HSO_3^-}) + q(\mathrm{SO_2}) \quad (13)$$

$$= \sqrt{K_{I1} K_{\mathrm{H}} p} + K_{\mathrm{H}} p. \quad (14)$$

Together with Eq. (1), we arrive at

$$k' = \frac{2\,RT}{r}\left(\frac{1}{2}\sqrt{\frac{K_{\mathrm{H}} K_{I1}}{p}} + K_{\mathrm{H}}\right). \quad (15)$$

This model yields a dependence on $k' \propto p^{-1/2}$ in the low concentration regime, but not for our data which were obtained at much higher concentrations than those used by Clegg and Abbatt (2001).

In cases where an adsorbing molecule dissociates upon adsorption the Langmuir isotherm takes a modified form (Crowley et al., 2010; Huthwelker et al., 2006):

$$\theta = \frac{q}{q_{\mathrm{S}}} = \frac{\sqrt{\frac{K_{\mathrm{H}} K_{I1} p}{q_{\mathrm{S}}^2}}}{1 + \sqrt{\frac{K_{\mathrm{H}} K_{I1} p}{q_{\mathrm{S}}^2}}}. \quad (16)$$

With Eq. (1) and adding the Henry adsorption term, it follows that

$$k' = \frac{2\,RT}{r}\left(\frac{\frac{K_{\mathrm{H}} K_{I1}}{q_{\mathrm{S}}}}{2\sqrt{\frac{K_{\mathrm{H}} K_{I1} p}{q_{\mathrm{S}}^2}}\left(\sqrt{\frac{K_{\mathrm{H}} K_{I1} p}{q_{\mathrm{S}}^2}} + 1\right)^2} + K_{\mathrm{H}}\right). \quad (17)$$

Model parameters $K_{\mathrm{H}} K_{I1}$ and q_{S} are determined by nonlinear regression. No temperature dependency on $K_{\mathrm{H}} K_{I1}$ is found. The dependency q_{S} on temperature is formulated by a van't Hoff-like expression; see Table 1. In addition, q_{S} is about 60 % larger for aged ice. However, the residuals of the fit are not normally distributed (Shapiro–Wilk normality test; $P = 0.04$).

Due to strong scatter, we are not able to find a significant temperature trend for K_{H} describing the physisorption of SO_2. To explore the temperature dependency on K_{H}, temperature-dependent measurements of k' were performed using higher concentrations with a partial pressure of around $p(SO_2) = 1$ Pa at the recorded peak maximum. In addition, the experimental setup was changed: instead of using the methylsilyl-deactivated column, an untreated fused silica column was used. We assumed that due to better wettability, ice deposition on the untreated silica surface results in a better surface coverage than in methylsilyl-deactivated columns. Furthermore, the coating procedure in these subsets of experiments was modified to minimize the length of the uncoated part of the column inside the cold box: after preparing the coating as described above, the cold box was opened and the uncoated tail of the column was manually drawn out of the box though a pinhole. This reduced the length of the uncoated tail in the cold box to about 30 cm. For further stabilization of the ice surface, the column was maintained for 3 h at 256 K after the coating procedure. After keeping the column at 207 K overnight, the chromatographic experiments were performed the next day. The ice film thickness was 6.5 µm. To find evidence for anomalous adsorption behavior of SO_2 caused by the formation of a quasi-liquid layer when approaching the melting point of water ice, the SF_6 / SO_2 chromatograms where measured up to 267 K. If a surface premelt layer acted like a supercooled liquid water film, SO_2 might dissolve in the layer, therefore enhancing the capacity ratio k' and therefore K_{H} when approaching the melting point. However, with one exception where the column erroneously had not been rinsed before with Milli-Q water and dried with synthetic air to remove soluble impurities, mainly NO_3^- ions, SF_6 and SO_2 peaks could not be separated at temperatures > 232 K. This implies that our results obtained with the untreated column are unaffected by a quasi-liquid layer at higher $p(SO_2)$, where k' is nearly independent of $p(SO_2)$. The results indicate that the dominant adsorption at higher $p(SO_2)$ which was investigated in our experiments is physisorption on the dry surface. In those cases where the measured peaks of SF_6 and SO_2 overlap, the true peak maxima were determined by fitting two exponential modified Gauss functions to the overlapping peaks (Felinger, 1994). Afterwards the peak maximum time of each peak was determined by a linear search algorithm. K_{H} at $p \to \infty$ is determined as an intercept by linear regression of k' vs. p^{-1} using Eq. (8).

In Fig. 4 the Henry's law adsorption constant $\ln K_{\mathrm{H}}$ obtained for ice-coated methylsilyl-deactivated columns and an ice-coated untreated column is plotted against $1/T$. With the

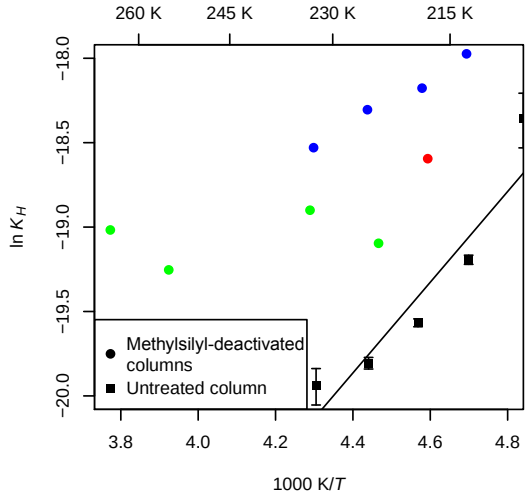

Figure 4. K_H as a function of T for experiments using an untreated column and methylsilyl-deactivated columns coated with aged ice. Experiments conducted with the same prepared column are marked by the same color.

van't Hoff equation,

$$\ln K_H = \ln K_H^{\infty} - \frac{\Delta H_a}{RT}, \tag{18}$$

no reasonable fit is possible for the experiments performed with methylsilyl-deactivated columns. Even in the case of the untreated column, the values of K_H systematically deviate from the van't Hoff plot regression line. Whereas K_H is weakly dependent on temperature using the methylsilyl-deactivated fused silica column, K_H decreases more strongly with temperature than when using an untreated fused silica column. A possible explanation for this might be that at higher temperatures formation of a quasi-liquid layer occurs at the interface of ice with the methylsilyl-deactivated fused silica surface.

3.2 Adsorption of acetone and *n*-hexane

To explore the possible impact of a quasi-liquid layer, the adsorption of acetone and *n*-hexane on an ice-coated methylsilyl-deactivated column was investigated in the temperature range 211–265 K. These compounds were selected because they are comparable in vapor pressure over a wide temperature range but differ in water solubility: *n*-hexane is insoluble in water, whereas acetone is miscible with water. Methane was used as an inert tracer. Figure 5 shows the chromatograms obtained using a methylsilyl-deactivated column coated with an ice film of 7.1 µm thickness. From left to right, the recorded peaks are from methane, *n*-hexane, and acetone. At peak maximum, the trace gas concentration ranged from 0.1 to 1.5 Pa for *n*-hexane and from 0.1 to 0.4 Pa for acetone. The *n*-hexane peaks are nearly symmetrical and the retention times are independent of the amounts injected, whereas

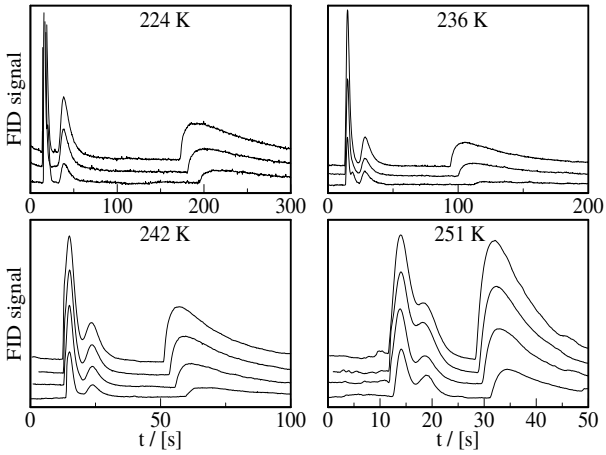

Figure 5. Chromatograms of a mixture of methane, *n*-hexane and acetone at different temperatures. The flow rate is 10 sccm. Methane is used as a non-adsorbable tracer.

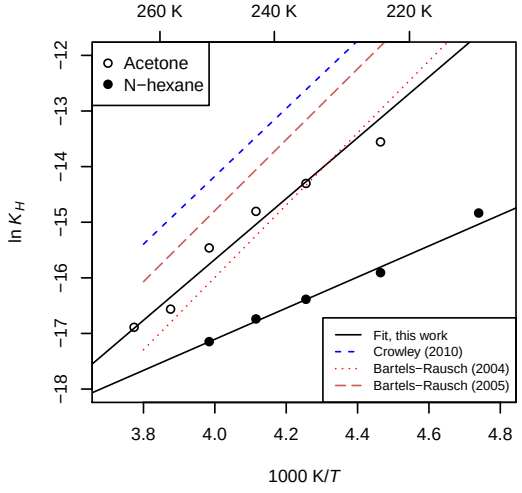

Figure 6. Van't Hoff plot of $\ln K_H$ vs. inverse temperature for adsorption of acetone and *n*-hexane on ice using a methylsilyl-deactivated fused silica column. The solid lines are fits of the data to Eq. (18), used to derive adsorption enthalpies. Van't Hoff plots of acetone from Bartels-Rausch et al. (2004a, b) and Bartels-Rausch et al. (2005) and recommended values from Crowley et al. (2010) extrapolated from lower temperatures to the temperature range investigated are shown for comparison.

the acetone peaks show some tailing with slightly increasing retention times with decreasing injection amounts, indicating that the slope of the isotherm is nonlinear. The adsorption of acetone on ice is described by a Langmuir adsorption isotherm according to Eq. (9); see the review by Crowley et al. (2010). Equation (10) is reorganized into a linear relation of $1/\sqrt{k'}$ vs. p:

$$\sqrt{\frac{2\,RT}{rk'}} = \frac{\sqrt{K_L}}{q_S}p + \frac{1}{\sqrt{K_L}}. \tag{19}$$

Table 2. Adsorption isotherm of *n*-hexane and acetone on ice

	$\ln(K_H^\infty/1\,\mathrm{mol\,m^{-2}\,Pa^{-1}})$	ΔH_a ($\mathrm{kJ\,mol^{-1}}$)
n-hexane	-28.3 ± 0.9	-23 ± 2
acetone	-37.6 ± 2.5	-45 ± 5

K_L of acetone is determined after linear regression from the intercept. For *n*-hexane, mean values of the retention times are determined for different injection amounts at one temperature. K_H of *n*-hexane is calculated using Eq. (5). The enthalpies of adsorption are determined using Eq. (18) by linear regression; see Fig. 6 and Table 2.

After obtaining the values of K_H, the surface coverage of *n*-hexane and acetone can be estimated at the lowest temperature investigated. Winkler et al. (2002) reported an adsorption capacity of $4.5 \times 10^{-6}\,\mathrm{mol\,m^{-2}}$ for acetone on ice. For *n*-hexane $\theta \approx 5\,\%$ at 1.5 Pa at 211 K and for acetone $\theta = 13\,\%$ at 0.4 Pa and 224 K are obtained for the largest concentrations observed at peak maximum. Therefore, it is concluded that the peak tailing of the acetone peaks is caused by partial saturation. Thus, it is justified to use Eq. (19) for extrapolation of K_L for $p \to 0$. However, additional causes for peak tailing like slow uptake may exist.

4 Discussion

4.1 Consistency of the peak maxima method

The consistency of the peak maxima method is checked by theoretical peak shape calculations using the R package ReacTran (Soetaert and Meysman, 2012); see Supplement Sect. S2 and Fig. 2b. When comparing locations of experimental peak maxima with peak maxima predicted by Eq. (1), it can be seen that at higher concentrations, the peak maxima are shifted towards longer retention times. As stated by Joensson and Loevkvist (1987), for Langmuir-like adsorption isotherms the accuracy of the peak maxima method is best for low to moderate concentrations. Hence, in case of nonlinear adsorption, the isotherm determined by the peak maxima method at higher concentration has to be regarded as the upper limit.

Slow uptake of SO_2 by diffusion into the ice surface is included into the 2-D model; see Fig. 2b. When taking diffusion into the ice surface into account, the peak maxima are shifted on the curve of Eq. (1) to higher retention times. In addition, the peak maxima are smaller and tailing is enhanced. As can bee seen from the simulation without including slow uptake (1-D model), Eq. (1) is nearly the envelope of the tails of the simulated peaks. This is used by the peak profile method (Huber and Gerritse, 1971) to determine the slope of the isotherm from a single peak tail. But, due to slow uptake into the surface, this method is not applicable for SO_2 on ice.

4.2 Comparison with literature

4.2.1 Adsorption of SO_2

The reanalysis of our experimental data reveals that the simple Langmuir adsorption isotherm is not suitable for the description of adsorption of SO_2 on ice. Only considering our data, either the Temkin model or the dissociative Langmuir model are more appropriate. When taking the results of Clegg and Abbatt (2001) and the chemical nature of SO_2 into account, we conclude that the adsorption is best described by the dissociative Langmuir model of Eq. (16) combined with simple physisorption described by Henry's adsorption isotherm. The experiments of Clegg and Abbatt (2001) were performed at lower SO_2 concentrations; thus saturation effects were not observed. SO_2 reaction with ice and dissociation is also supported by the study of Jagoda-Cwiklik et al. (2008) who investigated SO_2 adsorbates on the surface of ice nanoparticles at 128 K by FTIR spectroscopy: like in aqueous solutions, an HSO_3^- ion was found.

Crowley et al. (2010) reported a value of $K_{I1}K_H = 1.3 \times 10^{-13}\,\mathrm{mol^2\,m^{-4}\,Pa^{-1}}$ based on the data of Clegg and Abbatt (2001) for the model of Eq. (14) at 228 K. This value lies within the error limits of our value of $K_{I1}K_H = (7 \pm 5) \times 10^{-14}\,\mathrm{mol^2\,m^{-4}\,Pa^{-1}}$. A limitation of our study is that the experiments were performed at rather high SO_2 concentrations. This makes the determination of $K_{I1}K_H$ rather difficult, as can bee seen by a value of $P = 0.1$ for this fit parameter; see Table 1. Therefore, we are not able to find a temperature trend for $K_{I1}K_H$. This is in contrast to the observation of Clegg and Abbatt (2001) who found less uptake at lower temperatures.

The monolayer saturation capacity q_S of the dissociative Langmuir model describes the maximal adsorbed amount of SO_2 in one monolayer. Our values range from $9 \times 10^{-9}\,\mathrm{mol\,m^{-2}} = 5 \times 10^{11}\,\mathrm{cm^{-2}}$ at 205 K to $4 \times 10^{-8}\,\mathrm{mol\,m^{-2}} = 2 \times 10^{12}\,\mathrm{cm^{-2}}$ at 265 K; see Table 1. Taking $5 \times 10^{14}\,\mathrm{cm^{-2}}$ (Clegg and Abbatt, 2001) for the adsorption capacity of the normal ice surface as reference, dissociative adsorption of SO_2 must occur on active sites representing 0.1–0.5 % of the total surface. This result may be explained by surface premelting. At temperatures close to the melting point the ice surface may be regarded as a quasi-liquid layer where the hexagonal oxygen lattice is completely distorted. At temperatures below ≈ 260 K the oxygen lattice is distorted by point defects and the hydrogen bond network is distorted. Either vacancies in the outer bilayer predicted by molecular dynamics simulations (Bishop et al., 2009; Rikonen et al., 2014) or hydronium, hydroxide, and the Bjerrum L and D defects predicted by density functional theory calculations (Watkins et al., 2010) prevailing at the surface come into question as active sites for dissociative adsorp-

tion. D-defects at the surface, bearing a positive charge, possibly could attract HSO_3^- ions at the surface. Watkins et al. (2010) found by density functional calculation that surface D-defects form with a very small energy penalty of 0.06 eV. An activation energy of 11 kJ mol^{-1} = 0.11 eV for the formation of an active site can be derived from the model parameter a_2, describing the temperature dependency on q_S. Surprisingly for the hypothetical case of $T \to \infty$ K the saturation capacity approaches a limit of $q_s = 3 \times 10^{14}$ cm^{-2}.

One unanticipated finding is that q_S is larger for aged ice. A possible explanation for this might be that surface defects are more prevalent on the surface of aged ice. Another possible explanation for this is that the ice surface in our capillary columns increases during aging: shortly after preparation of the column, the inner wall is covered with individually frozen drops of water. During aging, the interstitial ice-free surface of the column is eventually covered with ice by desublimation from the frozen drops.

Besides the aging effect, other reasons for poor reproducibility of the properties of ice surfaces must exist. Whereas the reproducibility of the chromatograms of one column at one temperature is good, the reproducibility of experiments of two prepared columns is rather bad. There are several possible explanations for this result: the properties of the ice surface are also affected by the underlying surface properties of the fused silica column, which may influence cristallinity and surface defects.

4.2.2 Adsorption of acetone and *n*-hexane

In recent years, several studies concerning the adsorption of acetone on ice have been published; see the review of Crowley et al. (2010) and references therein. However, all these studies only covered the temperature range of 140–228 K. In this review, the results are summarized as an expression for the van't Hoff equation for Henry's law adsorption isotherm using Eq. (18). When extrapolating these expressions to the higher temperature range of our experiment, it is found that the isotherms of Bartels-Rausch et al. (2004a, b) and Bartels-Rausch et al. (2005) are closest to our measured values of Henry's adsorption isotherm constant; see Fig. 6. In the first study, breakthrough curves were measured using a column packed with ice beads, and in the second study, an ice-coated-wall flow tube was used. Bartels-Rausch et al. (2004a) and Bartels-Rausch et al. (2005) obtained an adsorption enthalpy of -52 ± 2 and -46 ± 3 kJ mol^{-1}, respectively. Our value of -45 ± 5 kJ mol^{-1} is slightly lower but complies with the error limits.

Bartels-Rausch et al. (2004a) determined the surface area available for adsorption by a Brunauer–Emmett–Teller (BET) analysis of methane adsorption isotherms. Bartels-Rausch et al. (2005) prepared the ice surface by slowly freezing water at the inner surface of a Pyrex flow tube. They assume that the ice surface corresponds to the geometric inner surface of the tube. Thus, in both experiments the surface of ice adsorbents is regarded as being known. These results suggest that within experimental uncertainty, the real ice surface in our column corresponds approximately to the geometric inner surface of the ice-coated part of the column, due to the consistency of our data concerning the adsorption of acetone with these studies. The temperature trend of the isotherms of Bartels-Rausch et al. (2004a) and Bartels-Rausch et al. (2005) extrapolates to higher temperatures up to 265 K. No visible change caused by a quasi-liquid layer is found in the temperature trend.

For *n*-hexane on pure ice, the enthalpy of adsorption has not been measured yet. Hoff et al. (1995) reported $\Delta H_a = -37.3 \pm 1.3$ kJ mol^{-1} for the adsorption on ice-coated Chromosorb P in the temperature range 263–273 K, which is much higher than our value of -23 ± 2 kJ mol^{-1}. For adsorption of *n*-hexane on liquid water, -28 kJ mol^{-1} was determined by Hartkopf and Karger (1973) at 286 K.

4.3 Atmospheric implications

The adsorbed fraction of a trace gas in a contrail or cirrus cloud with ice surface area density σ is given by

$$\frac{N_s}{N_g} = \frac{\sigma\ RT\ q}{p}. \tag{20}$$

In the case of Henry's adsorption isotherm of Eq. (4), we can write

$$\frac{N_s}{N_g} = \sigma\ RT\ K_H. \tag{21}$$

In the case of the model of Eq. (14) and of the dissociative Langmuir model of Eq. (16), we arrive at

$$\frac{N_s}{N_g} \approx \sigma\ RT \sqrt{\frac{K_{I1} K_H}{p}} \tag{22}$$

at low concentrations where physisorption of SO_2 by linear Henry's adsorption isotherm can be neglected. For cirrus clouds, values of $\sigma = 0.003$ m^{-1} were reported and for contrails, values of $\sigma = 0.003 - 0.012$ m^{-1} were reported by Schroeder et al. (2000). In an aircraft plume, SO_2 concentrations of $> 5 \times 10^8$ cm^{-3} were observed by Schumann et al. (1998). At 205 K the adsorbed fraction calculated with Eq. (22) is about 10^{-3} for $\sigma = 0.003$ m^{-1}. For acetone the adsorbed fraction according to Eq. (21) is about 10^{-4} at 205 K. These findings suggest that adsorption of SO_2 and acetone on ice particles in the plume of an aircraft and subsequent vertical transport by particle sedimentation is negligible.

Sokolov and Abbatt (2002) estimated an upper limit for the surface density of $\sigma = 0.1$ m^{-1} for tropospheric ice clouds. Here, the adsorbed fraction of SO_2 is about 0.3 at the same SO_2 concentration as above. Therefore, we conclude that interaction of SO_2 with ice is only important in very dense ice clouds.

5 Conclusions

Gas chromatography with water-ice-coated fused silica columns is a screening tool that is well suited to studying the adsorption of trace gases with weak or medium adsorption in the range $k' = 0.1 - 100$ ($K_H = 8 \times 10^{-9} - 8 \times 10^{-6}$ mol m^{-2}Pa^{-1}). By using a humidified carrier gas, the experiments can be performed at temperatures close below the melting point. Except the special low temperature coating box, only standard equipment for gas chromatography is required.

The interaction of SO_2 with ice surfaces in the temperature range 205–265 K is described by a dissociative Langmuir model in conjunction with weaker physisorption described by Henry's adsorption isotherm. No temperature trend for the adsorption equilibrium constant is found for the dissociative adsorption process. The monolayer saturation capacity for dissociative adsorption increases with increasing temperature and ice aging. Adsorption occurs on active sites representing 0.1–0.5 % of the total surface. These findings support the existence of surface premelting.

Slow uptake into the ice surface is evidenced by peak tailing in addition to tailing arising from the nonlinear isotherm.

The possible interference of the underlying bare or methylsilyl-deactivated column surface with the ice surface cannot be ruled out. Further work is required to find evidence as to whether ice films on untreated fused silica surfaces or on methylsilyl-deactivated fused silica surfaces are more likely to resemble the surface of atmospheric ice particles.

Code availability. The R code for simulation of chromatograms is provided in the Supplement.

Data availability. Measurement data are available upon request from the corresponding author (langenberg@uni-bonn.de).

The Supplement related to this article is available online at https://doi.org/10.5194/acp-18-7527-2018-supplement.

Author contributions. US suggested the experimental setup. SL performed the experiments, analyzed the data and drafted the manuscript.

Competing interests. The authors declare that they have no conflict of interest.

Acknowledgements. This work was supported by the "Deutsche Forschungsgemeinschaft (DFG)" within the DFG priority program "Basics of the Impact of Air and Space Transportation on the Atmosphere". We thank Thomas Huthwelker for helpful discussions.

Edited by: Christopher Hoyle
Reviewed by: three anonymous referees

References

Abbatt, J. P. D.: Interactions of Atmospheric Trace Gases with Ice Surfaces: Adsorption and Reaction, Chem. Rev., 103, 4783–4800, https://doi.org/10.1021/cr0206418, 2003.

Bartels-Rausch, T., Guimbaud, C., Gäggeler, H. W., and Ammann, M.: The partitioning of acetone to different types of ice and snow between 198 and 223 K, Geophys. Res. Lett., 31, L16110, https://doi.org/10.1029/2004GL020070, 2004a.

Bartels-Rausch, T., Guimbaud, C., Gäggeler, H. W., and Ammann, M.: Correction to "The partitioning of acetone to different types of ice and snow between 198 and 223 K", Geophys. Res. Lett., 31, L23106, https://doi.org/10.1029/2004GL021838, 2004b.

Bartels-Rausch, T., Huthwelker, T., Gaggeler, H. W., and Ammann, M.: Atmospheric pressure coated-wall flow-tube study of acetone adsorption on ice, J. Phys. Chem. A, 109, 4531–4539, https://doi.org/10.1021/jp045187l, 2005.

Bartels-Rausch, T., Jacobi, H.-W., Kahan, T. F., Thomas, J. L., Thomson, E. S., Abbatt, J. P. D., Ammann, M., Blackford, J. R., Bluhm, H., Boxe, C., Domine, F., Frey, M. M., Gladich, I., Guzmán, M. I., Heger, D., Huthwelker, Th., Klán, P., Kuhs, W. F., Kuo, M. H., Maus, S., Moussa, S. G., McNeill, V. F., Newberg, J. T., Pettersson, J. B. C., Roeselová, M., and Sodeau, J. R.: A review of air-ice chemical and physical interactions (AICI): liquids, quasi-liquids, and solids in snow, Atmos. Chem. Phys., 14, 1587–1633, https://doi.org/10.5194/acp-14-1587-2014, 2014.

Bartle, K., Wright, B., and Lee, M.: Characterization of glass, quartz, and fused silica capillary column surfaces from contact-angle measurements, Chromatographia, 14, 387, https://doi.org/10.1007/BF02262872, 1981.

Bishop, C. L., Pan, D., Liu, L. M., Tribello, G. A., Michaelides, A., Wang, E. G., and Slater, B.: On thin ice: surface order and disorder during pre-melting, Faraday Discuss, 141, 277–292, https://doi.org/10.1039/B807377P, 2009.

Chu, L., Diao, G., and Chu, L.: Heterogeneous Interactions of SO_2 on H_2O_2-Ice films at 190–210 K, J. Phys. Chem. A, 104, 7565–7573, https://doi.org/10.1021/jp001323k, 2000.

Clapsaddle, C. and Lamb, D.: The Sorption Behavior of SO_2 at Temperatures between −30°C and −5°C, Geophys. Res. Lett., 16, 1173–1176, https://doi.org/10.1029/GL016i010p01173, 1989.

Clegg, S. and Abbatt, J.: Uptake of Gas-Phase SO_2 and H_2O_2 by Ice Surfaces: Dependence on Partial Pressure, Temperature and Surface Acidity, J. Phys. Chem. A, 105, 6630–6636, https://doi.org/10.1021/jp010062r, 2001.

Conklin, M. and Bales, R.: SO_2 uptake on ice spheres: liquid nature of the ice-air interface, J. Geophys. Res., 98, 16851–16855, https://doi.org/10.1029/93JD01207, 1993.

Conklin, M., Sommerfeld, R., Laird, S., and Villinski, J.: Sulfur dioxide reactions on ice surfaces: implications for dry deposition to snow, Atmos. Environ., 27A, 159–166, https://doi.org/10.1016/0960-1686(93)90346-Z, 1993.

Crowley, J. N., Ammann, M., Cox, R. A., Hynes, R. G., Jenkin, M. E., Mellouki, A., Rossi, M. J., Troe, J., and Wallington, T. J.: Evaluated kinetic and photochemical data for atmospheric chemistry: Volume V – heterogeneous reactions on solid substrates, Atmos. Chem. Phys., 10, 9059–9223, https://doi.org/10.5194/acp-10-9059-2010, 2010.

Dash, J. G., Rempel, A. W., and Wettlaufer, J. S.: The physics of premelted ice and its geophysical consequences, Rev. Mod. Phys., 78, 695–741, https://doi.org/10.1103/RevModPhys.78.695, 2006.

Farwell, S. and Barinaga, C.: Sulfur-Selective Detection with the FPD: Current Enigmas, Practical Usage, and Future Directions, J. Chromatogr. Sci., 24, 483–494, https://doi.org/10.1093/chromsci/24.11.483, 1986.

Felinger, A.: Deconvolution of Overlapping Skewed Peaks, Anal. Chem., 66, 3066, https://doi.org/10.1021/ac00091a013, 1994.

Giddings, J.: Unified Separation Science, Wiley, 1991.

Hartkopf, A. and Karger, B. L.: Study of the interfacial properties of water by gas chromatography, Accounts of Chemical Research, 6, 209–216, https://doi.org/10.1021/ar50066a006, 1973.

Hoff, J., Wania, F., Mackay, D., and Gillham, R.: Sorption of Nonpolar Organic Vapors by Ice and Snow, Environ. Sci. Technol., 29, 1982–1989, https://doi.org/10.1021/es00008a016, 1995.

Huber, J. and Gerritse, R.: Evaluation of dynamic gas chromatographic methods for the determination of adsorption and solution isotherms, J. Chromatogr. A, 58, 137, https://doi.org/10.1016/S0021-9673(00)96607-X, 1971.

Huthwelker, T., Lamb, D., Baker, M., Swanson, B., and Peter, T.: Uptake of SO_2 by polycrystalline water ice, J. Coll. Int. Sci., 238, 147–159, https://doi.org/10.1006/jcis.2001.7507, 2001.

Huthwelker, T., Ammann, M., and Peter, T.: The Uptake of Acidic Gases on Ice, Chem. Rev., 106, 1375–1444, https://doi.org/10.1021/cr020506v, 2006.

Jagoda-Cwiklik, B., Devlin, J. P., and Buch, V.: Spectroscopic and computational evidence for SO_2 ionization on 128 K ice surface, Phys. Chem. Chem. Phys., 10, 4678–4684, https://doi.org/10.1039/B809839P, 2008.

Jönsson, J. A. and Lövkvist, P.: Determination of adsorption isotherms from chromatographic measurements, using the peak maxima method, J. Chromatogr. A, 408, 1–7, https://doi.org/10.1016/S0021-9673(01)81785-4, 1987.

Langenberg, S.: Anwendung der Kapillar-Gaschromatographie zur Untersuchung von Spurengas-Aerosolwechselwirkungen, Ph.D. thesis, Rheinische-Friederich-Wilhelms-Universität Bonn, http://d-nb.info/989933385/34, (last access: 23 April 2018), 1997.

Langenberg, S. and Schurath, U.: Ozone Destruction on Ice, Geophys. Res. Lett., 26, 1695–1698, https://doi.org/10.1029/1999GL900325, 1999.

Langenberg, S., Proksch, V., and Schurath, U.: Solubilities and Diffusion of trace gases in cold sulfuric acid films, Atmos. Environ., 32, 3129–3137, https://doi.org/10.1016/S1352-2310(97)00490-1, 1998.

Ogden, M. and McNair, H.: Characterization of fused-silica capillary tubing by contact angle measurements, J. Chromatogr., 354, 7–18, https://doi.org/10.1016/S0021-9673(01)87006-0, 1986.

R Core Team: R: A Language and Environment for Statistical Computing, R Foundation for Statistical Computing, Vienna, Austria, http://www.R-project.org/, (last access: 23 April 2018), 2016.

Riikonen, S., Parkkinen, P., Halonen, L., and Gerber, R. B.: Ionization of Acids on the Quasi-Liquid Layer of Ice, J. Phys. Chem. A, 118, 5029–5037, https://doi.org/10.1021/jp505627n, pMID: 24927623, 2014.

Schröder, F., Kärcher, B., Duroure, C., Ström, J., Petzold, A., Gayet, J.-F., Strauss, B., Wendling, P., and Borrmann, S.: On the Transition of Contrails into Cirrus Clouds, J. Atmos. Sci., 57, 464–480, https://doi.org/10.1175/1520-0469(2000)057<0464:OTTOCI>2.0.CO;2, 2000.

Schumann, U.: On the effect of emissions from aircraft engines on the state of the atmosphere, Ann. Geophys., 12, 365–384, https://doi.org/10.1007/s00585-994-0365-0, 1994.

Schumann, U., Schlager, H., Arnold, F., Baumann, R., Haschberger, P., and Klemm, O.: Dilution of aircraft exhaust plumes at cruise altitudes, Atmos. Environ., 32, 3097–3103, https://doi.org/10.1016/S1352-2310(97)00455-X, 1998.

Soetaert, K. and Meysman, F.: Reactive transport in aquatic ecosystems: Rapid model prototyping in the open source software R, Environmental Modelling & Software, 32, 49–60, https://doi.org/10.1016/j.envsoft.2011.08.011, 2012.

Sokolov, O. and Abbatt, J. P. D.: Adsorption to Ice of n-Alcohols (Ethanol to Hexanol), Acetic Acid, and Hexanal, J. Phys. Chem. A, 106, 775–782, https://doi.org/10.1021/jp013291m, 2002.

Sommerfeld, R. and Lamb, D.: Preliminary measurements of SO_2 adsorbed on ice, Geophys. Res. Lett., 13, 349–351, https://doi.org/10.1029/GL013i004p00349, 1986.

Walcek, C. J. and Pruppacher, H. R.: On the scavenging of SO_2 by cloud and raindrops: I. A theoretical study of SO_2 absorption and desorption for water drops in air, J. Atmos. Chem., 1, 269–289, https://doi.org/10.1007/BF00058732, 1983.

Watkins, M., VandeVondele, J., and Slater, B.: Point defects at the ice (0001) surface, PNAS, 107, 12429–12434, https://doi.org/10.1073/pnas.1001087107, 2010.

Wexler, A.: Vapor pressure formulation for ice, J. Res. Natl. Bur. Stand. A, 81, 5–20, https://doi.org/10.6028/jres.081a.003, 1977.

Winkler, A. K., Holmes, N. S., and Crowley, J. N.: Interaction of methanol, acetone and formaldehyde with ice surfaces between 198 and 223 K, Phys. Chem. Chem. Phys., 4, 5270–5275, https://doi.org/10.1039/B206258E, 2002.